Instantaneous Spectral Analysis

Jerrold Prothero, KM Zahidul Islam, Henry Rodrigues, Luciano Mendes, Jon Barrueco, Jon Montalban

Abstract—The standard Fourier Transform (FT) can be seen as a change of basis in which a "time domain" amplitude sequence is re-expressed as a sum of sinusoids with constant coefficients allowing for the spectral analysis of the signal. The FT can be employed either as a tool for studying the sinusoidal properties of the amplitude sequence, or more actively as a prescription for transmitting the amplitude sequence using some range of frequencies. Introduced here, Instantaneous Spectral Analysis (ISA) is similar to the FT in usage, except that ISA expresses an amplitude sequence in terms of sinusoids with continuously-varying amplitudes. This makes ISA more suitable than the FT for studying situations in which the amplitude sequence is generated by a continuously time-varying (non-ergodic) source, corresponding to a non-stationary spectrum. Viewed prescriptively, ISA allows an amplitude sequence to be compressed into a much smaller range of frequencies than the FT, essentially because ISA is not restricted by an assumption in the proof of the sampling theorem, that the spectrum is stationary over the evaluation interval. Intuitively, the FT expresses increasing time-domain detail by using increasingly higher frequencies. ISA, instead, uses an increasingly dense set of sinusoids with time-varying amplitude, within a fixed frequency range.

Index Terms—amplitude-varying sinusoid, instantaneous, spectral analysis.

I. INTRODUCTION

FOURIER analysis has been the standard tool for analyzing signals in the frequency domain. Using implementation-efficient variants, known as fast Fourier transforms (FFTs) [1], a handful of basic functions, such as the power spectrum and the cross power spectrum, are widely employed in signal analysis for different applications. The FFT algorithm is the key tool for analyzing a communication system's frequency and impulse responses, channel coherence bandwidth and signal amplitude and phase spectrum.

The Fourier transform (FT) can be abstractly viewed as representing signals by modulating a set of basis functions, specifically complex exponentials, resulting in a sum of circles on the complex plane, where the magnitude and initial phase of each circle are given by its corresponding coefficient. A known limitation of the FT is its spectral stationarity, since its coefficients are constants within the evaluation time-window. Furthermore, the FT inherently presents the paradigm in which the sampling period is inversely proportional to the bandwidth of its frequency domain basis functions.

Non-stationary signal analysis has been widely studied, with short-time Fourier transform (STFT) as the traditional

J. Prothero and Z. Islam are with Astrapi Corporation, USA. (e-mail:{jprothero, zislam}@astrapi-corp.com)

H. Rodrigues and L. Mendes are with National Institute of Telecommunications (Inatel), Brazil. (e-mail:{henry, luciano}@inatel.br)

J. Barrueco, J. Montalban are with TSR Reserch Lab, UPV/EHU, Spain. (e-mail:{jon.barrueco, jon.montalban}@ehu.eus)

method [2], generating the well-known spectrogram. This transformation is accomplished using a sliding time-window, with a trade-off between time and frequency resolution. Joint time-frequency distributions are an alternative technique for analyzing time-varying spectra, where Gabor [3], Ville [4], and Page [5] have established the main foundations in the area. The common idea is to derive a function, which depends on both time and frequency, that describes how the signal's energy intensity is simultaneously distributed in the time and frequency domains.

Although STFT and the vast number of joint time-frequency distributions [6] can handle non-stationarity, *all* existing frequency analysis techniques are bounded by the paradigm of requiring a higher basis bandwidth for representing a higher sampling frequency signal.

This paper proposes a novel non-stationary frequency analysis tool, called instantaneous spectral analysis (ISA), which represents waveforms as sinusoids with continuously time-varying amplitude within the evaluation period. These sinusoids can be represented using complex spirals that are generalizations of the complex circles used by the FT.

ISA conceptually differs from any other existing frequency analysis tool, including Fourier and time-frequency distributions, because it treats the time domain waveform as a polynomial or sequence of polynomials. Another difference between ISA and the conventional frequency analysis tools lies in the fact that the ISA basis functions are complex spirals, i.e., complex exponentials with continuously increasing or decreasing amplitude, as opposed to Fourier's (constant magnitude) complex circles. ISA is based on a generalization of Euler's formula, which produces continuously-varying amplitude complex exponentials, instead of the constant amplitude complex exponentials that support the FT. Finally, ISA presents a unique basis bandwidth compression characteristic: if the evaluation period is T seconds long, the ISA basis functions are strictly within a $\frac{1}{T}$ Hz bandwidth, regardless of the number of samples within the time-window. The ISA basis spectrum becomes more densely packed as the number of time domain samples increases.

This paper is structured as follows. Section II summarizes some well-known signal analysis tools in order to better contextualize the ISA algorithm introduced here. Section III introduces the ISA mathematical background and generalizes the known equivalence between the Taylor series representation of sinusoids and sums of complex circles. Section IV introduces the ISA algorithm and describes its characteristics. Section V describes discrete-time ISA with matrix notation. Section VI briefly describes ISA arithmetic complexity. Section VII compares ISA and the FT as spectrum measurement tools while Section VIII shows convergence between ISA and the FT for some signals of interest. Section IX concludes the

paper.

II. Signal analysis techniques

A set of signal analysis tools are reviewed in order to better contextualize the ISA algorithm introduced here. The best known frequency analysis tool is the FT, which has variants depending on the nature of the time and frequency domain signals, whether they are periodic or aperiodic, discrete-time or continuous-time.

The discrete-time Fourier transform (DTFT) creates a periodic and continuous frequency domain signal from an aperiodic discrete time signal [7]. Its direct form is given by

$$X(\omega) = \sum_{\aleph=0}^{N-1} x(\aleph)e^{-i\omega\aleph}, \tag{1}$$

where x is the N-samples input time domain signal with $\aleph$ being the sample index, and ω the continuous-frequency variable. Its inverse form is given by

$$x(\aleph) = \frac{1}{2\pi}\int_0^{2\pi} X(\omega)e^{i\omega\aleph}d\omega, \tag{2}$$

where the DTFT frequency domain content is composed by an infinite number of samples in the $[0, 2\pi]$ interval.

The most limited (and useful) version of the FT is the discrete Fourier transform (DFT). It is based on the idea of reassembling the time domain from a sampled version of the DTFT frequency domain. If $X(k)$ is the uniformly-spaced sampled version of $X(\omega)$, the minimum number of frequency samples needed to perfectly reconstruct $x(\aleph)$ is N [8], where $\omega = \frac{k}{2\pi}$ for $k = 0, 1, \ldots, N-1$. In other words, in order not to lose information from the time to frequency transformation, the minimum number of frequency components needs to be exactly the number of time domain samples, leading to the direct and inverse DFT given by

$$X(k) = \sum_{\aleph=0}^{N-1} x(\aleph)e^{-\frac{i2\pi k\aleph}{N}}, \tag{3}$$

and

$$x(\aleph) = \frac{1}{N}\sum_{k=0}^{N-1} X(k)e^{\frac{i2\pi k\aleph}{N}}, \tag{4}$$

respectively.

In order to analyze non-stationary signals, a wide set of time-frequency signal analysis tools [9], [10] are available. The most classical method is the STFT, for which the underlying idea is to divide a longer signal into a set of overlapping segments, with the FT applied on each segment, i.e., a sliding windowing process [11] given by

$$X(\omega, \tau) = \sum_{\aleph=-\infty}^{\infty} x(\aleph)\upsilon(\aleph - \tau)e^{-i\omega\aleph}, \tag{5}$$

where τ is the time-offset of the sliding window υ. The STFT is invertible [8] and is given by

$$x(\aleph) = \frac{1}{2\pi\upsilon(0)}\int_0^{2\pi} X(\tau, \omega)d\tau. \tag{6}$$

The spectrogram corresponds to the energy of $X(\omega, \tau)$, and presents a trade-off between time and frequency resolution [11].

Fractional Fourier transform (FRFT) is a generalization of the FT in the sense that a family of linear transformations can be sequentially applied, in order to obtain any intermediary domain between time and frequency [12]. It is defined as

$$\mathcal{F}_\alpha[x](u) = \sqrt{1 - i\cot(\alpha)}e^{i\pi\cot(\alpha)u^2}$$
$$\int_{-\infty}^{\infty} e^{-i2\pi(\csc(\alpha)ux - \frac{\cot(\alpha)}{2}x^2)}x(t)dt, \tag{7}$$

where t is the continuous time, u is interpreted as a linear combination between time and frequency, and α is the transform order (or angle) where $\alpha = \pi/2$ and $\alpha = 0$ corresponds to the classical FT and the identity operator, respectively. One of the FRFT applications is time-frequency representations [13], where the time-frequency domain gets rotated by the α parameter.

Time-frequency distributions [6] represent the signal energy across the time-frequency grid. The Wigner-Ville distribution is used for time-frequency representation, using the analytic version of the signal and is defined [14] as

$$\rho_x(\omega, t) = \int_{-\infty}^{\infty} x\left(t + \frac{\tau}{2}\right)x^*\left(t - \frac{\tau}{2}\right)e^{-i\omega\tau}d\tau. \tag{8}$$

It assumes that the input is a mono-component signal [15], which can be a significant limitation. Although is has synthesis applications [16], this representation is not invertible due to the presence of noise and crossterms [17], [18].

All previously presented signal analysis techniques are FT-based tools. They are therefore limited to the paradigm of requiring higher basis function bandwidth in order to represent a higher time resolution.

III. ISA mathematical background

The familiar Euler's formula

$$e^{it} = \cos(t) + i\sin(t) \tag{9}$$

can be generalized by raising the imaginary constant i on the left side to fractional powers. The new term, which is a contribution of this paper, is given by

$$e^{ti^{(2^{2-m})}}. \tag{10}$$

Notice that (10) reduces to the standard Euler's term in the special case $m = 2$.

Table I presents the generalized Euler's terms given by (10) assuming positive integer values of m.

TABLE I
GENERALIZED EULER'S TERMS AS A FUNCTION OF POSITIVE INTEGER
VALUES OF m.

m	0	1	2	3	4	5	$\ldots$
$e^{ti^{(2^{2-m})}}$	e^t	e^{-t}	e^{it}	$e^{t\sqrt{i}}$	$e^{t\sqrt[4]{i}}$	$e^{t\sqrt[8]{i}}$	$\ldots$

The standard Euler's formula in (9) can be expanded as a Taylor series and grouped into real and imaginary terms. The same procedure can also be used for each term in Table I to

derive a generalization of Euler's formula for integer $m \geq 0$, given by

$$e^{ti^{(2^{2-m})}} = \sum_{n=0}^{\lceil 2^{m-1}\rceil - 1} i^{n2^{2-m}} \psi_{m,n}(t), \qquad (11)$$

where $\lceil \cdot \rceil$ denotes the ceiling function and

$$\psi_{m,n}(t) = \sum_{q=0}^{\infty} (-1)^{q\lceil 2^{1-m}\rceil} \frac{t^{q\lceil 2^{m-1}\rceil + n}}{(q\lceil 2^{m-1}\rceil + n)!} \qquad (12)$$

are called the *Cairns series functions*. The proof of (11) provided in Appendix A shows the Cairns functions for $m = 0, 1, 2$ and 3. Notice that $\psi_{2,0}(t)$ and $\psi_{2,1}(t)$ give us the Taylor series for the standard cosine and sine functions, respectively.

Each value of m produces a set of functions $\psi_{m,n}(t)$; from the summation limits in (11), it can be seen that each set, or m-level, has a total of $\lceil 2^{m-1}\rceil$ functions. Fig. 1 depicts the $\psi_{m,n}(t)$ for $m = 0, 1, 2$, and 3.
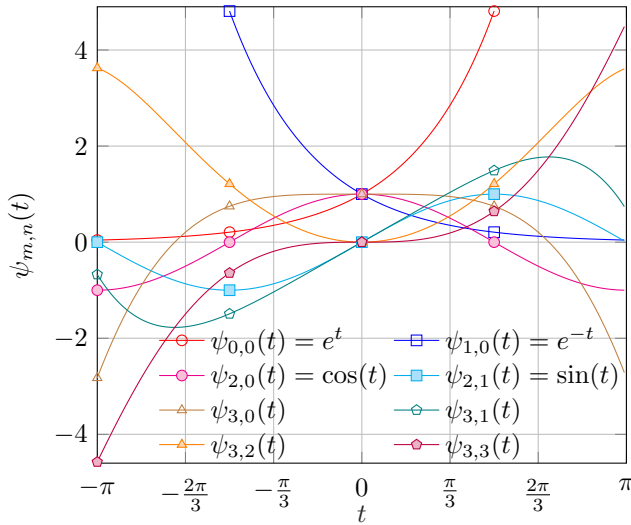
Fig. 1. Cairns functions.

An important property of the $\psi_{m,n}(t)$ is the regular pattern of their coefficients, as shown in Table II for $0 \leq m \leq M$ with $M = 3$.

TABLE II
CAIRNS SERIES COEFFICIENTS.

$\psi_{m,n}(t)$	1	t	$\frac{t^2}{2!}$	$\frac{t^3}{3!}$	$\frac{t^4}{4!}$	$\frac{t^5}{5!}$	$\frac{t^6}{6!}$	$\frac{t^7}{7!}$
$\psi_{0,0}(t) = e^t$	1	1	1	1	1	1	1	1
$\psi_{1,0}(t) = e^{-t}$	1	-1	1	-1	1	-1	1	-1
$\psi_{2,0}(t) = \cos(t)$	1	0	-1	0	1	0	-1	0
$\psi_{2,1}(t) = \sin(t)$	0	1	0	-1	0	1	0	-1
$\psi_{3,0}(t)$	1	0	0	0	-1	0	0	0
$\psi_{3,1}(t)$	0	1	0	0	0	-1	0	0
$\psi_{3,2}(t)$	0	0	1	0	0	0	-1	0
$\psi_{3,3}(t)$	0	0	0	1	0	0	0	-1

From Table II it is possible to conclude that the Cairns coefficients define a set of orthogonal vectors. Essentially, this is because within any m-level no two rows have nonzero entries in the same column, and across m-levels any column in which two rows have the same sign is matched by a column in which they have opposite sign.

More precisely, if M is a positive integer, then the vectors formed from the first 2^M coefficients of the functions $\psi_{m,n}(t)$ for $0 \leq m \leq M$ constitute a set of orthogonal basis vectors for a 2^M-dimensional space. These can be normalized to produce the orthonormal 2^M Cairns basis vectors.

The existence of the 2^M Cairns basis vectors implies that any Taylor polynomial $p(t)$ of degree $K < 2^M$ can be orthogonally projected onto polynomials formed from the first 2^M terms of the Cairns series functions simply by taking the inner product of $p(t)$'s coefficients with the 2^M Cairns basis vectors. The resulting coefficients $c_{m,n}$ for each Cairns basis function are referred to as the *projection coefficients*.

The first 2^M terms of the Cairns series functions $\psi_{m,n}(t)$ are only an approximation to the full infinite series expansion of the $\psi_{m,n}(t)$. However, the error in the approximation is $O(t^{(2^M)})$, with a reciprocal factorial coefficient, and therefore falls off very rapidly as M increases. For high-degree polynomials, therefore, it is reasonable to speak of projecting onto the $\psi_{m,n}(t)$ by this procedure.

It is well-known that the cosine and sine functions produced by Euler's formula can be represented not only by Taylor series, but also by sums of complex exponentials. Explicitly

$$\cos(t) = 1 - \frac{t^2}{2!} + \frac{t^4}{4!} - \frac{t^6}{6!} + \ldots = \frac{1}{2}\left(e^{it} + e^{-it}\right) \quad (13)$$

and

$$\sin(t) = t - \frac{t^3}{3!} + \frac{t^5}{5!} - \frac{t^7}{7!} + \ldots = \frac{1}{2i}(e^{it} - e^{-it}). \quad (14)$$

This characteristic also holds for a generalized exponential description, which can be defined as

$$E_{m,n}(t) = \frac{1}{\lceil 2^{m-1}\rceil} \sum_{p=0}^{\lceil 2^{m-1}\rceil - 1} i^{-n(2p+1)2^{2-m}} e^{ti^{(2p+1)2^{2-m}}}, \qquad (15)$$

where the $E_{m,n}(t)$ are called the *Cairns exponential functions*.

By expanding the right side of (15) as a sum of Taylor polynomials and recursively canceling terms, it is shown in Appendix B that for all m and n

$$E_{m,n}(t) = \psi_{m,n}(t). \qquad (16)$$

Equation (16) indicates that once a polynomial has been projected onto the Cairns series functions, it can be immediately converted into a sum of complex exponentials. This is useful for examining instantaneous spectral usage as shown in Section IV.

IV. ISA FORMULATION AND ITS CHARACTERISTICS

While frequency information is not readily apparent from the $\psi_{m,n}(t)$ representation, it can be determined precisely, and on an instant-by-instant basis, from the $E_{m,n}(t)$. Each $E_{m,n}(t)$ can be expressed as a sum of products, in which each term is the product of a complex gain-adjusted real-valued exponential with a complex circle (or sinusoid). The real-valued exponentials may be either rising or falling, and have different growth

constants in the exponent. The complex circles may rotate in either direction, and with different frequencies.

The ISA method introduced here could also be termed "spectral calculus", since it shares with differential calculus the property of replacing a discrete average with instantaneous information.

ISA takes as input any sequence of real or complex amplitude values (the "time domain"), each of which has a monotonically increasing time value associated with it. No further assumptions are required concerning the nature of this data, such as linear time-invariance (LTI).

As output, ISA returns a set of sinusoids of differing frequencies (the "frequency domain"), each of which has continuously time-varying amplitude. Summing the product of each sinusoid with its amplitude allows the time domain to be precisely reconstructed at each point in time.

The key steps of ISA are as follows:

1) Fit a Taylor polynomial to an input sequence of real-valued or complex-valued amplitudes. (Alternately, if a polynomial is available from some other means, that may be used as well.)

2) Project the polynomial onto the Cairns series functions, generating the projection coefficients $c_{m,n}$. At this point, any Taylor polynomial $p(t)$ of order $K-1$ with $K = 2^M$ can be synthesized as

$$p(t) = \sum_{m=0}^{M} \sum_{n=0}^{\lceil 2^{m-1} \rceil - 1} c_{m,n} \psi_{m,n}(t). \qquad (17)$$

3) Convert from the Cairns series functions $\psi_{m,n}(t)$ to the Cairns exponential functions $E_{m,n}(t)$.

4) Combine frequency information contained within the Cairns exponential functions to identify a sum of sinusoids with continuously time-varying amplitudes.

The ISA representation can be used to correctly re-generate the input amplitude sequence, by summing the complex gain-weighted amplitude information associated with each frequency, confirming that the two representations are equivalent.

For each sinusoid identified, its amplitude gives the spectral usage of the input sequence at the sinusoid's frequency as a continuous function of time. In this way, it becomes possible to define instantaneous spectrum usage.

To describe Step 4 of the ISA algorithm in more detail, using the identity $e^{i\pi/2} = i$ the generalized Euler's term $e^{ti(2^{2-m})}$ can be expressed as

$$e^{ti(2^{2-m})} = e^{t\cos(\pi 2^{1-m})} e^{it\sin(\pi 2^{1-m})}, \qquad (18)$$

as proved in Appendix C.

With a slight modification, (18) allows us to represent (15) equivalently as (19) (below), which can be subdivided into three distinct factors:

1) $e^{it\sin(\pi(2p+1)2^{1-m})}$ is a unit circle in the complex plane with frequency given by

$$f_{m,p} = \frac{\sin(\pi(2p+1)2^{1-m})}{2\pi}. \qquad (20)$$

2) $e^{t\cos(\pi(2p+1)2^{1-m})}$ is a real-valued exponential with growing or decaying magnitude depending on the m, p combination.

3) $i^{-n(2p+1)2^{2-m}}$ is a complex constant with unitary magnitude causing a constant phase rotation.

The following further observations from (19) are noteworthy:

• For $m = 0$ and $m = 1$ the frequency factor is equal to the constant one, since the sine function evaluates to zero.

• For $m \geq 2$, no two distinct m levels will contain the same frequencies, since $\sin(\pi(2p+)2^{1-m})$ depends on m.

• The same frequencies appears in $E_{m,n}(t)$ across all n at level m, since $\sin(\pi(2p+1)2^{1-m})$ does not depend on n.

Since both $\sin(\pi(2p+1)2^{1-m})$ and $\cos(\pi(2p+1)2^{1-m})$ can switch sign depending on the value of p, it follows that for $m \geq 2$ each positive frequency will be matched by an equal negative frequency, and for $m \geq 3$ each positive and negative frequency will appear twice, i.e., for two different values of p, with both a rising and falling exponential as its real-valued amplitude coefficient. These observations may be perceived from Fig. 2, which shows the frequency value of each complex sinusoid as a function of m and p.

At this point, any sequence (fitted as a polynomial) can be described as (21) (below). In this new representation, a sum of complex sinusoids with constantly varying envelope (given by the real-valued exponentials) are weighted by Cairns coefficients (which are input sequence dependent). It is the real-valued exponential terms that provides the ISA non-stationary characteristic, since the frequency domain content is not purely determined by constants, but by continuously-varying amplitudes.

In order to find the instantaneous amplitude of each frequency, all terms of (19) that have the same frequency need to be algebraically assembled. For $m \leq 2$, $E_{m,n}(t)$ this leads to well-known special cases

$$E_{0,0}(t) \quad = e^t, \qquad (22)$$

$$E_{1,0}(t) \quad = e^{-t}, \qquad (23)$$

$$E_{2,0}(t) \quad = \cos(t) = \frac{1}{2} \left(e^{-it} + e^{it} \right), \qquad (24)$$

$$E_{2,1}(t) \quad = \sin(t) = \frac{i}{2} \left(e^{-it} - e^{it} \right). \qquad (25)$$

Substituting (19) into (17), using the equivalence between the Cairns exponential functions and the Cairns series functions, then associating terms corresponding to complex sinusoids with the same frequency, leads to (26). Considering the evaluation time to be $0 \leq t \leq T$, the first, second, third, and fourth terms corresponds to complex sinusoids with frequencies equal to $f_{DC} = 0$ (DC component), $f_{max} = \frac{1}{T}$ (maximum), $f_{min} = -\frac{1}{T}$ (minimum), and $-\frac{1}{T} < f < \frac{1}{T}$, respectively. This results in a unique ISA characteristic: the frequency domain complex sinusoids basis functions are always contained within the frequency range $-\frac{1}{T} \leq f \leq \frac{1}{T}$. In other words, the basis bandwidth depends only on the evaluation time T and is independent of the number of samples within the evaluation time. As the number of samples increases, the

JOURNAL OF COMMUNICATION AND INFORMATION SYSTEMS, VOL. 34, NO.1, 2019.

16

$$E_{m,n}(t) = \frac{1}{\lceil 2^{m-1} \rceil} \sum_{p=0}^{\lceil 2^{m-1} \rceil - 1} i^{-n(2p+1)2^{2-m}} e^{t \cos(\pi(2p+1)2^{1-m})} e^{it \sin(\pi(2p+1)2^{1-m})} \tag{19}$$

$$p(t) = \sum_{m=0}^{M} \sum_{n=0}^{\lceil 2^{m-1} \rceil - 1} \overbrace{\frac{c_{m,n}}{\lceil 2^{m-1} \rceil}}^{\text{constant}} \sum_{p=0}^{\lceil 2^{m-1} \rceil - 1} \overbrace{i^{-n(2p+1)2^{2-m}}}^{\text{constant}} \overbrace{\overbrace{e^{t \cos(\pi(2p+1)2^{1-m})}}^{\text{real-valued exponential}} \overbrace{e^{it \sin(\pi(2p+1)2^{1-m})}}^{\text{complex sinusoid}}}^{\text{complex spiral}} \tag{21}$$
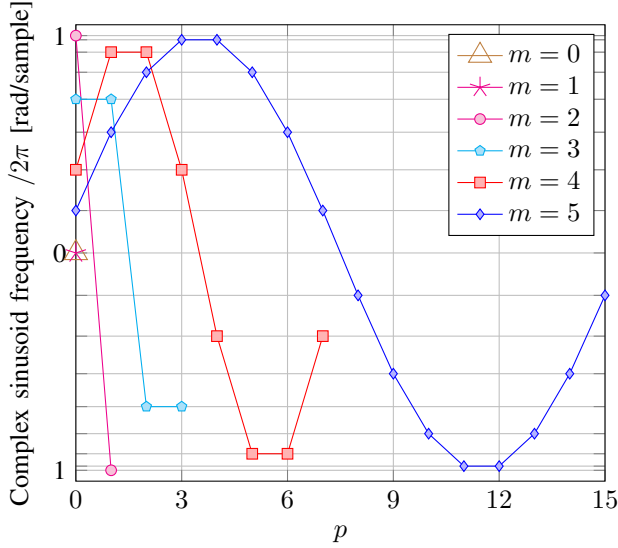
Fig. 2. ISA spectral component frequencies.

ISA spectrum is compressed, becoming more densely packed within the same limits.

As seen in Fig. 2, for $m \geq 3$ there are two values of p that generates the same complex sinusoid frequency. Working with the summation in p of (26) in order to group unique complex sinusoid frequencies $f_{m,p}$ for all combinations of m and p leads to (27), where $\langle \cdot \rangle_N$ denotes a modulo N operation.

Since the complex sinusoid frequency values do not depend on n, the summation order of n and p was reversed. Hence, the modulating or instantaneous amplitude associated with each complex sinusoid explicitly appears between the square brackets of (27) and can be defined at every distinct time t over its evaluation interval.

The polynomial $p(t)$ can be reconstructed from the ISA representation to arbitrary precision. The precision is limited by the size of the Cairns projection table, since ISA depends on the equivalence between the Cairns series and Cairns exponential functions, which are only exactly identical in the limit of an infinite number of polynomial terms. As a practical matter, a polynomial projected onto the Cairns projection table complete through $m = 4$ (implying 15th degree polynomials) will allow ISA to reconstruct the source polynomial with less than 1% error at every point in a region of $\pm \pi$ around the origin.

V. DISCRETE-TIME ISA WITH MATRIX NOTATION

This Section describes ISA using a compact matrix notation. Define a Taylor series basis matrix

$$\mathbf{B} = [\mathbf{b}_0 \, \mathbf{b}_1 \, \cdots \, \mathbf{b}_{K-1}] \tag{28}$$

with $\mathbf{B} \in \mathbb{R}^{N \times K}$ and

$$\mathbf{b}_k = \left[\frac{t_0^k}{k!} \, \frac{t_1^k}{k!} \, \cdots \, \frac{t_{N-1}^k}{k!} \right]^T, \tag{29}$$

where $\mathbf{b}_k \in \mathbb{R}^{N \times 1}$ corresponds to the kth-order term of the Taylor series with the discrete-time variable defined as $t_\aleph = \frac{2\pi}{N-1}(\aleph - \pi)$ with samples indexes $\aleph = 0, 1, \ldots, N - 1$. A sequence $x = [x_0, x_1, \cdots, x_{N-1}]^T$ with $x \in \mathbb{C}^{N \times 1}$ can be represented by a Taylor polynomial using

$$\mathbf{x} = \mathbf{B}\mathbf{h}, \tag{30}$$

where $\mathbf{h} \in \mathbb{C}^{K \times 1}$ are the polynomial coefficients. The equality in (30) holds for $K = N$, i.e., when it is guaranteed to be a polynomial of order $K - 1$ that perfectly fits a set of K samples. It is only possible to make $N > K$ when $\mathbf{x}$ represents a Taylor polynomial of order $K-1$ evaluated over N samples, representing an interpolated polynomial.

Considering that the summation of (12) has an infinite number of terms and the Taylor series basis of (30) is limited to K terms, the resulting Cairns series basis is given by

$$\mathbf{\Psi} = \mathbf{B}\mathbf{C}, \tag{31}$$

where $\mathbf{\Psi} \in \mathbb{R}^{N \times K}$ is an approximation of $\psi_{m,n}(t)$, and $\mathbf{C} \in \mathbb{R}^{K \times K}$ is the Cairns series coefficients matrix transposed with respect to the way it was shown in Table II.

Alternatively, $\mathbf{x}$ can be represented by the weighted linear combination of the Cairns series functions, i.e., the columns of $\mathbf{\Psi}$, by writing

$$\mathbf{\Psi}\mathbf{c} = \mathbf{x}, \tag{32}$$

where $\mathbf{c} \in \mathbb{R}^{K \times 1}$ are the *projection coefficients*. Notice (32) is equivalent to (17). The coefficients, $\mathbf{c}$, can be calculated as

$$\mathbf{B}\mathbf{C}\mathbf{c} = \mathbf{B}\mathbf{h}$$
$$\mathbf{c} = \mathbf{C}^{-1}\mathbf{h}. \tag{33}$$

$$p(t) = \overbrace{(c_{0,0}e^t + c_{1,0}e^{-t}) \cdot 1}^{f=0 \ (\text{DC})} + \overbrace{\left(c_{2,0}\frac{1}{2} - c_{2,1}\frac{i}{2}\right)e^{it}}^{f=\frac{1}{T} \ (\text{maximum})} + \overbrace{\left(c_{2,0}\frac{1}{2} + c_{2,1}\frac{i}{2}\right)e^{-it}}^{f=-\frac{1}{T} \ (\text{minimum})} + \overbrace{\sum_{m=3}^{M}\sum_{n=0}^{\lceil 2^{m-1}\rceil-1} c_{m,n}E_{m,n}(t)}^{-\frac{1}{T}<f<\frac{1}{T}} \qquad (26)$$

$$p(t) = \left[c_{0,0}e^t + c_{1,0}e^{-t}\right] + \left[c_{2,0}\frac{1}{2} - c_{2,1}\frac{i}{2}\right]e^{it} + \left[c_{2,0}\frac{1}{2} + c_{2,1}\frac{i}{2}\right]e^{-it} +$$

$$\sum_{m=3}^{M}\sum_{p=3\cdot 2^{m-3}}^{5\cdot 2^{m-3}-1}\left[\sum_{n=0}^{2^{m-1}-1}\frac{c_{m,n}}{2^{m-1}}\left(\frac{e^t\cos(\pi(2(\langle p\rangle_{(2^{m-1})}+1)2^{1-m})}{i^{n(2\langle p\rangle_{(2^{m-1})}+1)2^{2-m}}} + \frac{e^{-t}\cos(\pi(2(\langle p\rangle_{(2^{m-1})}+1)2^{1-m})}{i^{n(2(-p+3\cdot 2^{m-2})+1)2^{2-m}}}\right)\right]e^{it\sin(\pi(2(\langle p\rangle_{(2^{m-1})}+1)2^{1-m})} \qquad (27)$$

VI. ISA ARITHMETIC COMPLEXITY

An arithmetic complexity analysis is presented for each of the ISA steps, in terms of number of complex multiplications.

1) Fit a Taylor polynomial. If the polynomial of interest is already available, this step is obviously free in terms of algorithmic complexity. If the input data is a sequence of amplitude values, a polynomial must be fit. The standard way to do a polynomial fit involves matrix inversion which is $\mathcal{O}(N^3)$, where N is the number of input samples.

2) Project the polynomial coefficients onto the Cairns series functions. This step is represented by (33), where $\mathbf{C}^{-1}$ can be pre-calculated independently of the input sequence and contains $(M+1)2^M$ real-valued non-zero elements. Considering that the real-by-complex multiplication complexity is half that of complex-by-complex, this step has arithmetic complexity of $(M+1)2^{(M-1)}$.

3) Convert from Cairns series functions to Cairns exponential functions. This is simply a re-labeling, due to the identity between these two sets of functions, so it has no computational cost.

4) Group the ISA terms corresponding to the same frequencies. Grouping is an additive operation, so it should not be interpreted as requiring multiplications. However, the modulating trajectories, i.e., the time-varying spectral components are calculated by multiplying the projection coefficients $c_{m,n}$ with the complex constants and real-valued exponentials. The constants and real-valued exponentials of (21) can be pre-calculated. Assuming the polynomial will be evaluated at N points, this process takes $N\left(1 + \sum_{m=3}^{M}\sum_{n=0}^{2^{m-1}-2}2^{m-1} - 1\right)$ complex multiplications, for $M \geq 3$.

Therefore, the overall ISA analysis complexity is $N^3 + (M+1)2^{(M-1)} + N\left(1 + \sum_{m=3}^{M}\sum_{n=0}^{2^{m-1}-2}2^{m-1} - 1\right)$ for $M \geq 3$. Table III shows numeric values for $0 \leq M \leq 6$.

VII. COMPARISON BETWEEN ISA AND FT

A. Data Transmission Using Polynomials

Any signal can be described as a polynomial, which provides a smooth curve through some set of transmitted amplitude values. The signal can be real or complex-valued, where

TABLE III
ISA ARITHMETIC COMPLEXITY IN TERMS OF COMPLEX MULTIPLICATIONS.

Max. Cairns function level M	0	1	2	3	4	5	6
Number of samples N	1	2	4	8	16	32	64
Step 1 complex multiplications	0	8	64	512	4,096	32,768	262,144
Step 2 complex multiplications	0	2	6	16	40	96	224
Step 4 complex multiplications	0	0	4	80	944	9,088	79,680
Total complex multiplications	0	10	74	608	5,080	41,952	342,048

the resulting polynomial coefficients are real or complex-valued, respectively. Using ISA, any signal transmitted in time T can be constructed using only sinusoids with smoothly time-varying amplitudes and with frequencies of $\frac{1}{T}$ or less. Fig. 3 shows an example of an arbitrary sequence of 16 samples which is fitted by a 15th degree polynomial with a transmission time of 1 μs to be analyzed in the ISA domain.
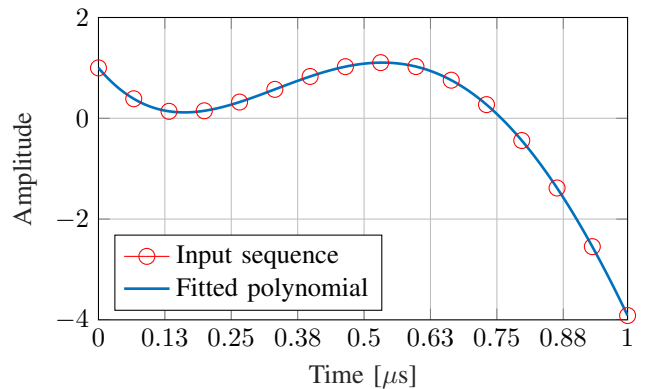
Fig. 3. Input sequence and fitted polynomial in time domain.

Applying the procedure described in Section IV, the ISA

spectral content was obtained and is shown in Fig. 4. The spectral component amplitudes vary continuously over the evaluation time and are composed entirely of frequencies of 1 MHz or less. Fig. 5 displays a snapshot of the instantaneous
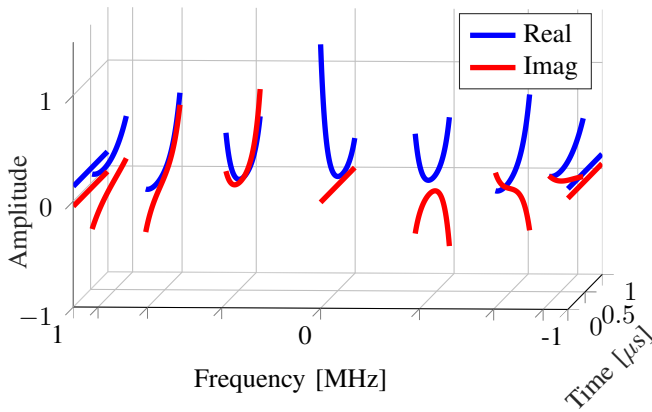
Fig. 4. ISA non-stationary spectral content of arbitrary 15th degree polynomial.

amplitude values for the 9 sinusoids used to construct the polynomial at time $t = 0.3$ μs. The ISA construction of the
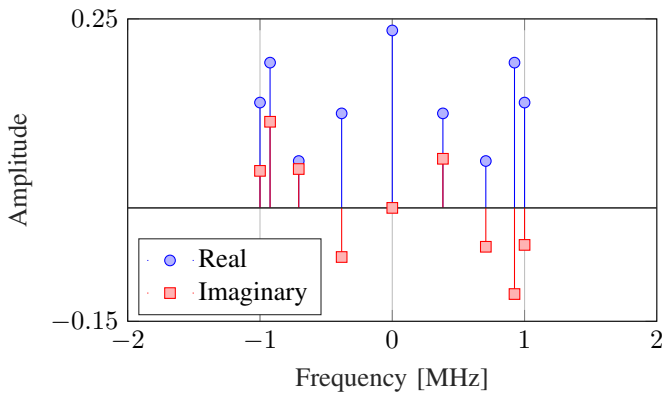
Fig. 5. Instantaneous polynomial spectrum at time $t = 0.3$ μs, i.e., a snapshot of the non-stationary spectral content of Fig. 4 at $t = 0.3$ μs.

polynomial agrees with direct evaluation of the polynomial, generated from its coefficients, to less than 1% error across the entire evaluation interval.

B. Frequency components bandwidth

The frequency components, or subcarriers, of both the FT and ISA are composed of complex sinusoids, i.e., complex circles in the complex plane. An analysis is made of bandwidth, considering it to be defined as the difference between the maximum and minimum complex sinusoid frequencies.

The bandwidth of the FT frequency components depends on the sampling frequency F_s, where according to the sampling theorem [19] the bandwidth is $\frac{F_s}{2}$ and F_s for real-valued and complex-valued signals, respectively. For a fixed sampling frequency, the evaluation time in FT influences only the subcarrier spacing but not the bandwidth.

ISA presents the opposite behavior to the FT. As mentioned in Section IV, the bandwidth of ISA frequency components depends only on the evaluation interval, and not on the sampling frequency, i.e., the number of samples within the evaluation interval. In the limit, a sequence with an infinite number of independent samples, within an interval with T seconds, produces ISA frequency components contained within a bandwidth of $\frac{1}{2T}$ and $\frac{1}{T}$ for real-valued and complex-valued samples, respectively. For a fixed evaluation time, the sampling frequency in ISA influences only the subcarrier density but not the bandwidth. Notice that the ISA subcarrier spacing is not uniform.

In Fig. 3, an arbitrary polynomial of degree 15 specifies 16 independent amplitude values. The FT power plot in Fig. 6, for the polynomial shown in Fig. 3, shows power usage with very limited roll-off from 1 MHz to 10 MHz. By contrast, the
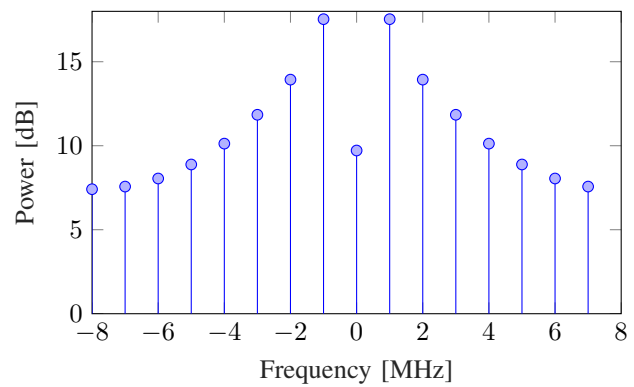
Fig. 6. FT average power spectrum.

ISA representation of the polynomial shown in Fig. 7 has no sinusoid with power outside of 1 MHz.
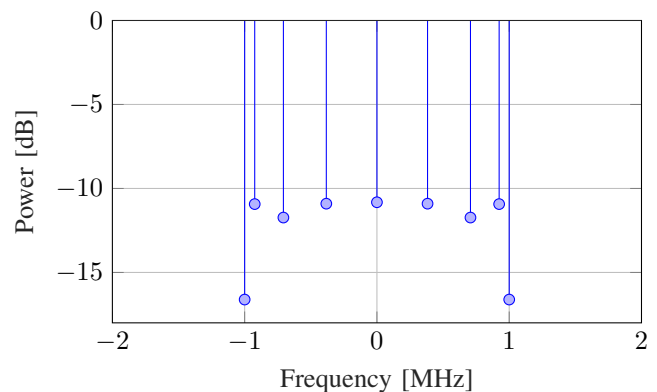
Fig. 7. ISA average power spectrum.

Traditionally, bandwidth has been defined by what is produced by an FT. Actually, however, an FT only specifies the range of frequencies and their amplitudes if the underlying time domain signal is represented using sinusoids with constant amplitude. ISA makes it possible to construct a signal using a much smaller frequency range by using continuously varying sinusoid amplitudes.

C. ISA spectral components

The complex exponential term $e^{it \sin(\pi(2p+1)2^{1-m})}$ of (19) has constant magnitude and thus describes a circle in the complex plane. The combination of p and m values generate unique frequencies called "ISA spectral components" that present some distinct characteristics when compared with the FT. Considering a time domain sequence of N samples, the DFT generates N frequency domain components. With ISA, the number of unique frequency components for $M \geq 2$ is given by

$$N_f = 1 + 2 \sum_{m=2}^{M} \lceil 2^{m-3} \rceil \qquad (34)$$

where $M = \log_2 N$. Fig. 8 shows the number of spectral components with respect to the number of time domain samples for both analysis tools. ISA has a smaller number of components
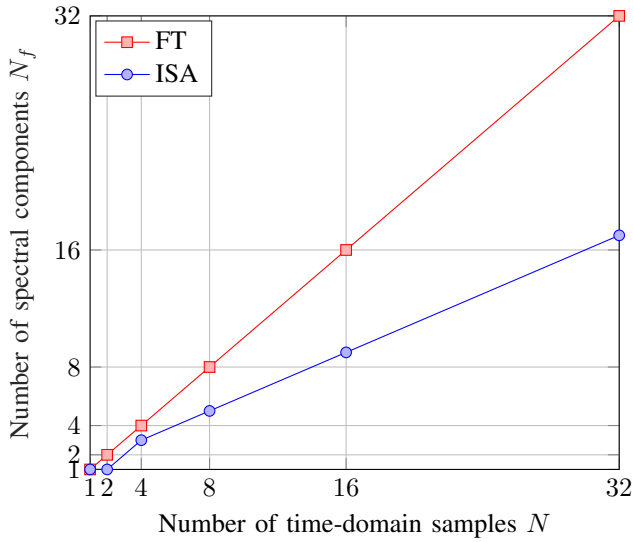
Fig. 8. Comparison between FT and ISA in terms of number of spectral components versus number of time domain samples.

which asymptotically tends to $N/2$ as $N \to \infty$. Notice that the comparison is based on the number of frequency components, not on the number of time domain samples. As each frequency component of ISA is continuously varying its amplitude over time, the number of samples of each frequency component is infinite, just as $p(t)$ has an infinite number of samples it the interval $0 \leq t \leq T$.

Second, the frequency of DFT components are located within the $[-\pi, \pi)$ rad/sample interval, i.e., it uses frequencies $2\pi k/N$ where $k = -\frac{N}{2}, \cdots, -1, 0, 1, \cdots, \frac{N}{2} - 1$. For ISA, the spectral components are always located within the interval corresponding to the Fourier components with $k = \pm 1$, independent of N. In other words, the higher the N value, the more densely packed the ISA spectral components become. Fig. 9 depicts an example for $N = 32$ and arbitrarily-valued spectral components.

Finally, the FT and ISA spectral components differ in that the ISA components are not linearly distributed within its interval $\left[\frac{-2\pi}{N}, \frac{2\pi}{N} \right)$ rad/sample. This occurs because its frequency values are derived from (20), which are sine-function
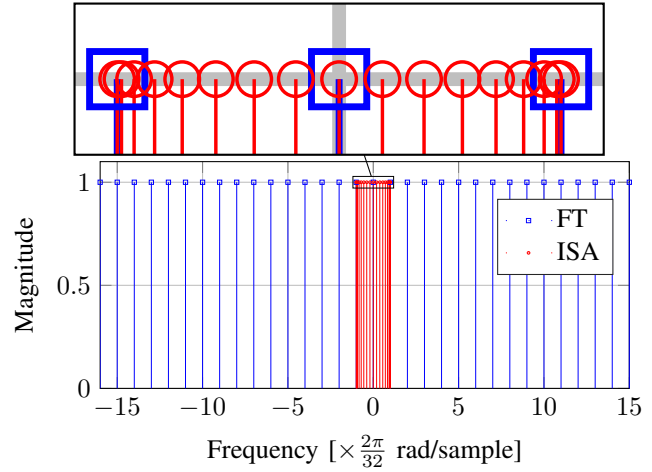
Fig. 9. Spectral components comparison for 32 samples time domain sequence.

dependent. Fig. 10 shows this behavior with an example for $N = 32$.
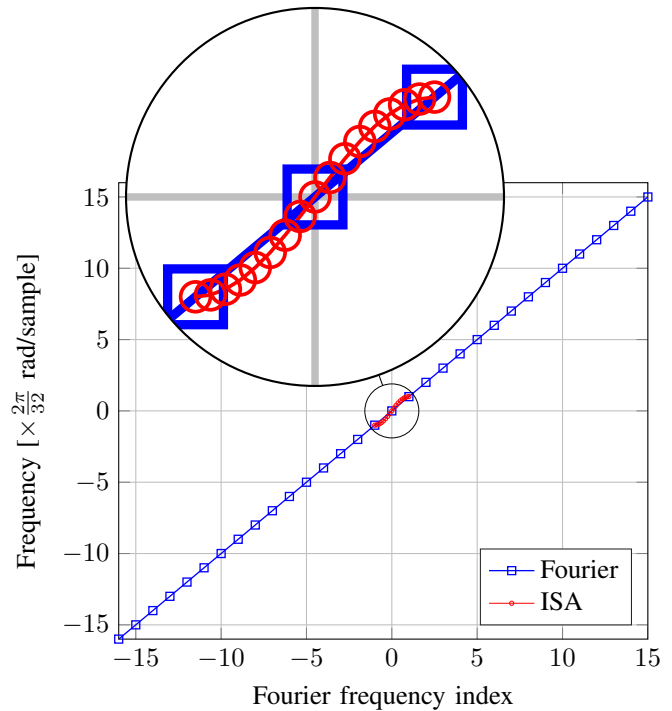
Fig. 10. Spectral components for 32 samples time domain sequence comparison.

D. Graphical interpretation

Both the ISA and FT synthesis tools may be interpreted as multi-carrier modulation schemes. In a generic multi-carrier modulation scheme, each (unmodulated) subcarrier is multiplied by a modulating signal, generating the modulated subcarrier. Finally, all modulated subcarriers are added to obtain the overall modulated signal. With the DFT, each of the N complex sinusoids in the basis corresponds to an unmodulated subcarrier; the frequency domain coefficients are

modulating signals, which in this case are constants within the evaluation time; the complex sinusoids multiplied by the coefficients correspond to the modulated subcarriers; finally, all modulated subcarriers are combined to correspond to the modulated (or synthesized) signal. ISA follows the same pattern, except that the modulating signals are not constants, but time-varying signals.

An arbitrary time domain signal was used to graphically demonstrate the difference between ISA and FT in terms of modulating and modulated signals. The signal was obtained by applying an inverse DFT to a 16-sample frequency domain vector, where each sample corresponds to a point in the 16-QAM constellation. ISA was also applied to this time domain signal for comparison. Fig. 11 depicts these signals for both ISA and FT.

In Fig. 11(a) and 11(c), the (complex) modulating signals are shown over time. With FT, these are straight lines corresponding to the constants in the 16-QAM constellation. For ISA, the modulating signals are not constants, and thus describe trajectories in the complex plane, where the marks '∗' and '○' corresponds to the start and end of the trajectories, respectively. Finally, the modulated signals resulting from multiplication of the modulating signals with its corresponding complex sinusoids are shown on 11(b) and 11(d).

Notice that the time domain overall modulated signal is exactly the same for both cases. However, the frequency domain representation is analyzed in two completely different ways.

E. Basis orthogonality

The matrix notation for Fourier synthesis is given by

$$\mathbf{F}\tilde{\mathbf{x}} = \mathbf{x}, \tag{35}$$

where $\tilde{\mathbf{x}} = [\tilde{x}_0, \tilde{x}_1, \cdots, \tilde{x}_{N-1}]^T$ is the stationary frequency domain representation of $\mathbf{x}$, and $\mathbf{F} = \frac{1}{\sqrt{N}}[\mathbf{f}_0, \mathbf{f}_1, \cdots, \mathbf{f}_{N-1}]$ is the DFT matrix with

$$\mathbf{f}_\aleph = \left[e^{i\aleph t_0}, e^{i\aleph t_1}, \cdots, e^{i\aleph t_{N-1}}\right]^T. \tag{36}$$

The FT has an orthogonal time domain basis since $\mathbf{F}^H\mathbf{F} = \mathbf{I}$. Going back from the time to frequency domain with the FT is straightforward since

$$\mathbf{x} = \mathbf{F}^{-1}\mathbf{x} = \mathbf{F}^H\mathbf{x} \tag{37}$$

The ISA basis is not an orthogonal linear transformation since Ψ is not unitary.

F. Symmetry

When either the real or imaginary parts of the underlying input sequence $\mathbf{x}$ are constant, e.g. purely real amplitudes, the FT exhibits the Hermitian symmetry property for real-valued time domain sequences. ISA also holds the same property, e.g., for a purely real input sequence, the fitted Taylor polynomial and the projection coefficients are also purely real, resulting in the symmetry

$$a_f(t) = a^*_{-f}(t), \tag{38}$$
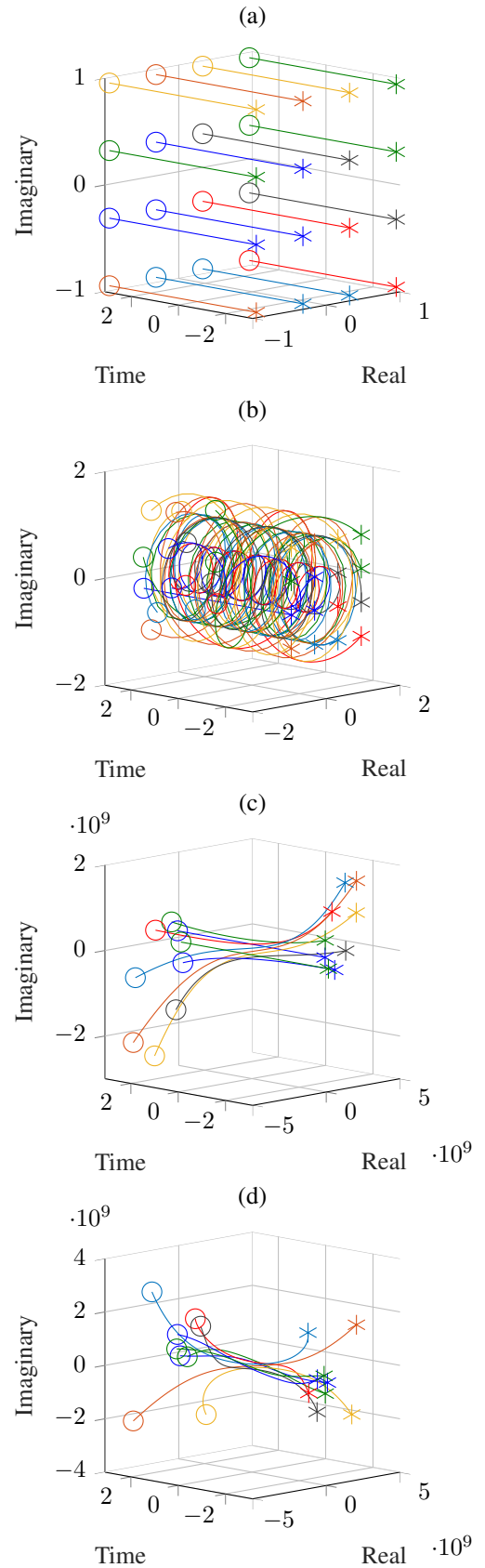
Fig. 11. Comparison between FT and ISA: (a) FT modulating signals; (b) FT modulated signals; (c) ISA modulating signals; (d) ISA modulated signals.

where $(\cdot)^*$ denotes the conjugate operator. This property arises in ISA because every positive frequency is paired with a negative frequency in the same Cairns exponential function, and because they are in the same Cairns exponential function, they will have the same projection coefficient, and therefore the same weight, resulting in cancellation of their paired complex components and addition of their paired real components. This means that the modulated signal for a given positive frequency f is the complex conjugate of its negative frequency counterpart. This can be seen in Fig. 12, which shows the ISA modulating trajectories for: (a) purely real input sequence and; (b) complex input sequence. It means that the single side band spectrum contains all the information for a purely real sequence.
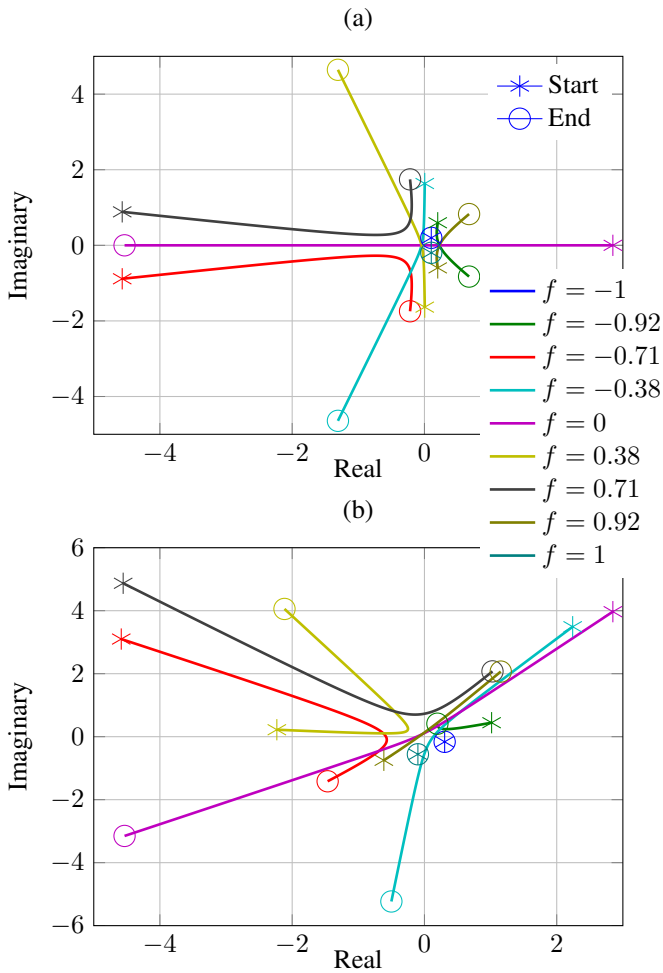
Fig. 12. Modulating trajectories with (a) non-symmetrical characteristic for complex-valued time domain samples and (b) conjugate symmetry for purely real samples. Legend represents the ISA frequency components with units in MHz.

In the example of Section VII-A, a purely real input sequence evaluated over a 1 μs interval generated ISA frequency components that occupy only 1 MHz, because the negative part of the spectrum is redundant due to Hermitian symmetry. When the input sequence is complex-valued, the negative part of the spectrum becomes non-redundant, making the ISA basis functions bandwidth 2 MHz wide. The bandwidth is doubled

because it is now representing double the information, i.e., a non-constant imaginary part.

VIII. CONVERGENCE OF ISA AND FT

ISA is more general than the FT in that the ISA can accurately represent a non-stationary spectrum characterized by sinusoids with continuously-varying amplitude. However, for simple cases characterized by constant-amplitude sinusoids, the ISA and FT representations converge.

The special case signals $\cos(t_\aleph)$, $\sin(t_\aleph)$, $e^{(i\frac{t_\aleph}{N})}$, and $e^{(-i\frac{t_\aleph}{N})}$ can be represented by Taylor polynomials with coefficients

$$
\begin{aligned}
\mathbf{h}_{\cos} &= \begin{bmatrix} 1 & 0 & -1 & 0 & 1 & 0 & -1 & 0 & \cdots \end{bmatrix}^{\mathrm{T}} \\
\mathbf{h}_{\sin} &= \begin{bmatrix} 0 & 1 & 0 & -1 & 0 & 1 & 0 & -1 & \cdots \end{bmatrix}^{\mathrm{T}} \\
\mathbf{h}_{e+} &= \begin{bmatrix} 1 & i & -1 & i & 1 & i & -1 & i & \cdots \end{bmatrix}^{\mathrm{T}} \\
\mathbf{h}_{e-} &= \begin{bmatrix} 1 & -i & -1 & -i & 1 & -i & -1 & -i & \cdots \end{bmatrix}^{\mathrm{T}},
\end{aligned}
\tag{39}
$$

respectively. After projecting these sequences into the Cairns space, the resulting coefficients are given by

$$
\begin{aligned}
\mathbf{c}_{\cos} &= \begin{bmatrix} 0 & 0 & 1 & 0 & 0 & 0 & 0 & 0 & \cdots \end{bmatrix}^{\mathrm{T}} \\
\mathbf{c}_{\sin} &= \begin{bmatrix} 0 & 0 & 0 & 1 & 0 & 0 & 0 & 0 & \cdots \end{bmatrix}^{\mathrm{T}} \\
\mathbf{c}_{e+} &= \begin{bmatrix} 0 & 0 & 1 & i & 0 & 0 & 0 & 0 & \cdots \end{bmatrix}^{\mathrm{T}} \\
\mathbf{c}_{e-} &= \begin{bmatrix} 0 & 0 & 1 & -i & 0 & 0 & 0 & 0 & \cdots \end{bmatrix}^{\mathrm{T}}.
\end{aligned}
\tag{40}
$$

Substituting (40) into (26) results in the synthesized signals

$$
\begin{aligned}
p_{\cos}(t_\aleph) &= \frac{1}{2}e^{it_\aleph} + \frac{1}{2}e^{-it_\aleph} & (41) \\
p_{\sin}(t_\aleph) &= -\frac{i}{2}e^{it_\aleph} + \frac{i}{2}e^{-it_\aleph} & (42) \\
p_{e+}(t_\aleph) &= e^{it_\aleph} & (43) \\
p_{e-}(t_\aleph) &= e^{-it_\aleph}. & (44)
\end{aligned}
$$

Therefore, in these cases, the ISA spectral content (modulating signals) corresponds exactly to the DFT spectral content.

An example is given in Fig. 13, where a single sinusoid of 1 MHz is measured by the FT and ISA. Although there are amplitude differences between the FT and ISA representations, both show only a frequency component of 1 MHz.

IX. CONCLUSIONS

ISA is a new technique for converting from an amplitude sequence through a polynomial into sinusoids with continuously-varying amplitude. A similar technique has not previously been available. It distinguishes from the FT, which converts an amplitude sequence into sinusoids with constant amplitude. ISA supports a conceptual model in which signals can be thought of as polynomials. Since a sequence of K amplitude values is equivalent to a unique polynomial of degree $K-1$, ISA provides a clean way to translate between the discrete-time viewpoint that a signal is a sequence of amplitude values, and the analog view that signals have to be transmitted as continuous waveforms. FT and ISA can reconstruct the same amplitude sequence, and are equivalent in terms of their time
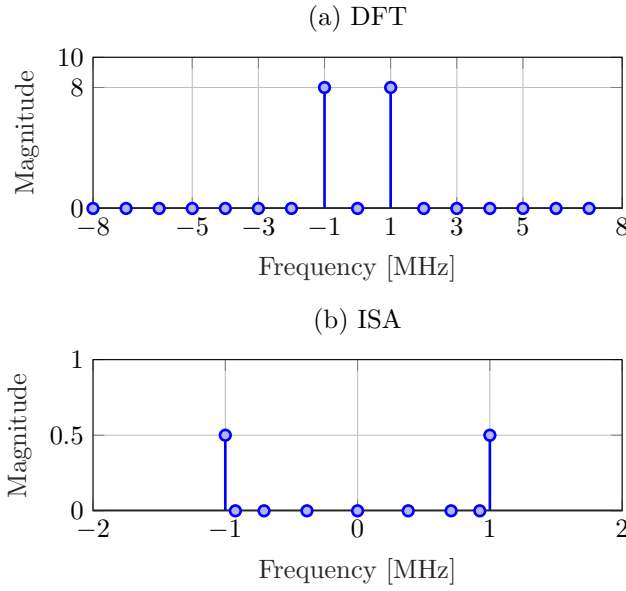
Fig. 13. Convergence of FT and ISA analysis for a cosine wave.

domain representations. However, their frequency representations are quite different. As shown, the number of frequency components is smaller than the DFT and strictly contained within a bandwidth which depends only on the symbol time duration, and not on the number of samples within that time window, i.e., the ISA spectrum becomes more densely packed as the number of time domain samples increases within a given evaluation interval. With ISA, it is possible to construct signals using only sinusoids in a limited frequency range that can convey many times more independent amplitude values (and therefore information) than is possible with standard signal modulation. Furthermore, the amplitude of ISA frequency components continuously vary with time, creating the non-stationary characteristic from which the instantaneous spectral analysis name arose.

This paper covered only the theoretical aspects of ISA. It's applications are under study, such as building an ISA-based modulation scheme [20]. Potentially, the ISA frequency domain basis bandwidth compression property could be an advantage for this new modulation scheme, by providing higher spectral efficiency when compared with conventional digital modulation schemes. Time-frequency representation is another possible application, not aiming at the substitution of existing techniques, but offering a new one from a new perspective.

X. Acknowledgment

The idea of applying a generalization of Euler's formula to telecommunications was introduced by John Cairns [21], [22].

XI. Patents

Astrapi holds foundational issued and pending patents related to ISA technology, including [23], [24], [25], [20].

Appendix A
Proof of Generalized Euler's Formula Taylor Series Interpretation

We show that for integer $m \geq 0$

$$e^{ti(2^{2-m})} = \sum_{n=0}^{\lceil 2^{m-1} \rceil - 1} i^{n2^{2-m}} \psi_{m,n}(t), \qquad (A.1)$$

where

$$\psi_{m,n}(t) = \sum_{q=0}^{\infty} (-1)^{q \cdot \lceil 2^{1-m} \rceil} \cdot \frac{t^{q \cdot \lceil 2^{m-1} \rceil + n}}{(q \cdot \lceil 2^{m-1} \rceil + n)!}. \qquad (A.2)$$

Three special cases of this identity are well-known, as shown below. For $m = 0$, (A.1) becomes

$$e^t = \psi_{0,0}(t) \qquad (A.3)$$

For $m = 1$, (A.1) becomes

$$e^{-t} = \psi_{1,0}(t) \qquad (A.4)$$

For $m = 2$, (A.1) becomes

$$e^{it} = \sum_{n=0}^{1} i^n \psi_{2,n}(t) = \psi_{2,0}(t) + i\psi_{2,1}(t) \qquad (A.5)$$

The general case of (A.1) can be proved by expanding $e^{ti(2^{2-m})}$ as a Taylor polynomial and grouping terms. This proceeds as follows.

$$e^{ti(2^{2-m})} \equiv \sum_{q=0}^{\infty} \frac{(ti(2^{2-m}))^q}{q!} \qquad (A.6)$$

Notice that when $q = 2^{m-1}$, we have

$$i^{q(2^{2-m})} = i^2 = -1. \qquad (A.7)$$

This tells us that every $q = 2^{m-1}$ steps the pattern of $i^{q(2^{2-m})}$ will repeat, with alternating sign. Since we are interested in grouping terms with like powers of i, we want to separate the series into subseries with terms separated by the step size. This gives us (roughly)

$$e^{ti(2^{2-m})} = \sum_{n=0}^{2^{m-1}-1} i^{n2^{2-m}} \sum_{q=0}^{\infty} (-1)^q \frac{t^{q \cdot 2^{m-1}+n}}{(q \cdot 2^{m-1}+n)!}. \qquad (A.8)$$

This is correct except for the case $m = 0$, which corresponds to e^t. We have two problems for $m = 0$: these are that $2^{m-1} = 1/2$ (we would like it to equal 1); and that the sign should not alternate for e^t. These problems can be fixed by adjusting (A.8) as

$$e^{ti(2^{2-m})} = \sum_{n=0}^{\lceil 2^{m-1} \rceil - 1} i^{n2^{2-m}} \sum_{q=0}^{\infty} (-1)^{q \cdot \lceil 2^{1-m} \rceil}$$
$$\cdot \frac{t^{q \cdot \lceil 2^{m-1} \rceil + n}}{(q \cdot \lceil 2^{m-1} \rceil + n)!} \qquad (A.9)$$

If we label the second summation $\psi_{m,n}(t)$ then we have (A.1) and (A.2).

We have seen that (A.9) or, equivalently, (A.1) and (A.2) reduces to familiar cases for $m = 0$, $m = 1$, and $m = 2$. As an example of an unfamiliar case, consider $m = 3$. We then have

$$e^{ti(2^{2-3})} = \sum_{n=0}^{\lceil 2^{3-1}\rceil - 1} i^{n2^{2-3}} \sum_{q=0}^{\infty} (-1)^{q\cdot\lceil 2^{1-3}\rceil} \cdot \frac{t^{q\cdot\lceil 2^{3-1}\rceil + n}}{(q\cdot\lceil 2^{3-1}\rceil + n)!}, \tag{A.10}$$

which simplifies to

$$e^{ti\frac{1}{2}} = \sum_{n=0}^{3} i^{\frac{n}{2}} \sum_{q=0}^{\infty} (-1)^{q\cdot 1} \cdot \frac{t^{q\cdot 4+n}}{(q\cdot 4+n)!}$$
$$= (1 - \frac{t^4}{4!} + \frac{t^8}{8!} - \dots) + i^{\frac{1}{2}}(t - \frac{t^5}{5!} + \frac{t^9}{9!} - \dots) + \tag{A.11}$$

APPENDIX B
EQUIVALENCE PROOF FOR CAIRNS EXPONENTIAL AND SERIES FUNCTIONS

We show here that the Cairns series functions

$$\psi_{m,n}(t) = \sum_{q=0}^{\infty} (-1)^{q\cdot\lceil 2^{1-m}\rceil} \cdot \frac{t^{q\cdot\lceil 2^{m-1}\rceil + n}}{(q\cdot\lceil 2^{m-1}\rceil + n)!} \tag{B.1}$$

are equivalent to the Cairns exponential functions

$$E_{m,n}(t) = \frac{1}{\lceil 2^{m-1}\rceil} \sum_{p=0}^{\lceil 2^{m-1}\rceil - 1} i^{-n(2p+1)2^{2-m}} e^{ti(2p+1)2^{2-m}}. \tag{B.2}$$

That is,

$$E_{m,n}(t) = \psi_{m,n}(t). \tag{B.3}$$

Four special cases of this identity are well-known, as shown below. For $m = 0$ and $n = 0$, (B.3) becomes

$$E_{0,0}(t) = e^t = \psi_{0,0}(t) = 1 + t + \frac{t^2}{2!} + \frac{t^3}{3!} + \dots. \tag{B.4}$$

For $m = 1$ and $n = 0$, (B.3) becomes

$$E_{1,0}(t) = e^{-t} = \psi_{1,0}(t) = 1 - t + \frac{t^2}{2!} - \frac{t^3}{3!} + \dots. \tag{B.5}$$

For $m = 2$ and $n = 0$, (B.3) becomes

$$E_{2,0}(t) = \frac{1}{2}(e^{it} + e^{-it}) = \cos(t) = \psi_{2,0}(t) = 1 - \frac{t^2}{2!} + \frac{t^4}{4!} - \dots. \tag{B.6}$$

For $m = 2$ and $n = 1$, (B.3) becomes

$$E_{2,1}(t) = \frac{1}{2}(i^{-1}e^{it} + i^{-3}e^{-it}) = \sin(t) = \psi_{2,1}(t)$$
$$= t - \frac{t^3}{3!} + \frac{t^5}{5!} - \dots. \tag{B.7}$$

It may be seen by inspection of (B.2) that $E_{m,n+1}(t)$ is the integral of $E_{m,n}(t)$, with constant of integration zero. This is similarly true for $\psi_{m,n}(t)$, as can be seen either directly from (B.1) or by examining the polynomial sequences expanded in Appendix A.

Therefore, to prove (B.3) it is sufficient to prove the case for $n = 0$

$$E_{m,0}(t) = \psi_{m,0}(t), \tag{B.8}$$

as equality for all other values of n will follow from parallel integration.

The proof of (B.8) follows from expanding $E_{m,0}(t)$ as a sum of Taylor series and recursively canceling terms. This proceeds as follows

$$E_{m,0}(t) = \frac{1}{\lceil 2^{m-1}\rceil} \sum_{p=0}^{\lceil 2^{m-1}\rceil - 1} e^{ti(2p+1)2^{2-m}}$$

$$E_{m,0}(t) = \frac{1}{\lceil 2^{m-1}\rceil} \sum_{p=0}^{\lceil 2^{m-1}\rceil - 1} \sum_{q=0}^{\infty} \frac{(ti(2p+1)2^{2-m})^q}{q!}. \tag{B.9}$$

Using an idea similar to Appendix A, we break the summation into subseries in which the terms are separated by a step size of 2^{m-1}. With the new index variable being n, this gives us

$$E_{m,0}(t) = \frac{1}{\lceil 2^{m-1}\rceil}$$
$$\sum_{n=0}^{\lceil 2^{m-1}\rceil - 1} \sum_{p=0}^{\lceil 2^{m-1}\rceil - 1} \sum_{q=0}^{\infty} \frac{(ti(2p+1)2^{2-m})^{\lceil 2^{m-1}\rceil q+n}}{(\lceil 2^{m-1}\rceil q + n)!}. \tag{B.10}$$

Now, separate out the imaginary factor

$$E_{m,0}(t) = \frac{1}{\lceil 2^{m-1}\rceil} \sum_{n=0}^{\lceil 2^{m-1}\rceil - 1} \sum_{p=0}^{\lceil 2^{m-1}\rceil - 1} \sum_{q=0}^{\infty}$$
$$\left[(i^{(2p+1)2^{2-m}})^{\lceil 2^{m-1}\rceil q+n}\right] \frac{t^{\lceil 2^{m-1}\rceil q+n}}{(\lceil 2^{m-1}\rceil q + n)!}. \tag{B.11}$$

If we look at the case $n = 0$ by itself, the right side of (B.11) becomes

$$\frac{1}{\lceil 2^{m-1}\rceil} \sum_{p=0}^{\lceil 2^{m-1}\rceil - 1} \sum_{q=0}^{\infty} [(i^{(2p+1)2^{2-m}})^{\lceil 2^{m-1}\rceil q}] \frac{t^{\lceil 2^{m-1}\rceil q}}{(\lceil 2^{m-1}\rceil q)!}$$

$$= \frac{1}{\lceil 2^{m-1}\rceil} \sum_{p=0}^{\lceil 2^{m-1}\rceil - 1} \sum_{q=0}^{\infty} [i^{2q(2p+1)}] \frac{t^{\lceil 2^{m-1}\rceil q}}{(\lceil 2^{m-1}\rceil q)!}$$

$$= \frac{1}{\lceil 2^{m-1}\rceil} \sum_{p=0}^{\lceil 2^{m-1}\rceil - 1} \sum_{q=0}^{\infty} [i^{4qp}i^{2q}] \frac{t^{\lceil 2^{m-1}\rceil q}}{(\lceil 2^{m-1}\rceil q)!}$$

$$= \frac{1}{\lceil 2^{m-1}\rceil} \sum_{p=0}^{\lceil 2^{m-1}\rceil - 1} \sum_{q=0}^{\infty} (-1)^q \frac{t^{\lceil 2^{m-1}\rceil q}}{(\lceil 2^{m-1}\rceil q)!}$$

$$= \frac{1}{\lceil 2^{m-1}\rceil} \lceil 2^{m-1}\rceil \sum_{q=0}^{\infty} (-1)^q \frac{t^{\lceil 2^{m-1}\rceil q}}{(\lceil 2^{m-1}\rceil q)!}$$

$$= \sum_{q=0}^{\infty} (-1)^q \frac{t^{\lceil 2^{m-1}\rceil q}}{(\lceil 2^{m-1}\rceil q)!}$$

$$= \psi_{m,0}(t). \tag{B.12}$$

This shows that the $n = 0$ subseries of (B.11) satisfies $E_{m,0}(t) = \psi_{m,0}(t)$. The proof of (B.3) therefore depends on

the $n > 0$ subseries of (B.8) summing to precisely zero. We show that next.

Removing the $n = 0$ subseries from (B.8), we have

$$\frac{1}{\lceil 2^{m-1} \rceil} \sum_{n=1}^{\lceil 2^{m-1} \rceil - 1} \sum_{p=0}^{\lceil 2^{m-1} \rceil - 1} \sum_{q=0}^{\infty}$$

$$\left[\left(i^{(2p+1)2^{2-m}} \right)^{\lceil 2^{m-1} \rceil q + n} \right] \frac{t^{\lceil 2^{m-1} \rceil q + n}}{(\lceil 2^{m-1} \rceil q + n)!}. \tag{B.13}$$

Next, we simplify the complex factor

$$= \frac{1}{\lceil 2^{m-1} \rceil} \sum_{n=1}^{\lceil 2^{m-1} \rceil - 1} \sum_{p=0}^{\lceil 2^{m-1} \rceil - 1} \sum_{q=0}^{\infty}$$

$$\left[i^{2q(2p+1)} i^{n(2p+1)2^{2-m}} \right] \frac{t^{\lceil 2^{m-1} \rceil q + n}}{(\lceil 2^{m-1} \rceil q + n)!}$$

$$= \frac{1}{\lceil 2^{m-1} \rceil} \sum_{n=1}^{\lceil 2^{m-1} \rceil - 1} \sum_{p=0}^{\lceil 2^{m-1} \rceil - 1} \sum_{q=0}^{\infty}$$

$$\left[i^{4qp} i^{2q} i^{n(2p+1)2^{2-m}} \right] \frac{t^{\lceil 2^{m-1} \rceil q + n}}{(\lceil 2^{m-1} \rceil q + n)!} \tag{B.14}$$

$$= \frac{1}{\lceil 2^{m-1} \rceil} \sum_{n=1}^{\lceil 2^{m-1} \rceil - 1} \sum_{p=0}^{\lceil 2^{m-1} \rceil - 1} \sum_{q=0}^{\infty}$$

$$\left[(-1)^q i^{n(2p+1)2^{2-m}} \right] \frac{t^{\lceil 2^{m-1} \rceil q + n}}{(\lceil 2^{m-1} \rceil q + n)!}.$$

Now, split (B.14) into two parts by dividing the p summation in half

$$= \frac{1}{\lceil 2^{m-1} \rceil} \sum_{n=1}^{\lceil 2^{m-1} \rceil - 1} \sum_{p=0}^{\lceil 2^{m-2} \rceil - 1} \sum_{q=0}^{\infty}$$

$$(-1)^q i^{n(2p+1)2^{2-m}} \frac{t^{\lceil 2^{m-1} \rceil q + n}}{(\lceil 2^{m-1} \rceil q + n)!} +$$

$$\frac{1}{\lceil 2^{m-1} \rceil} \sum_{n=1}^{\lceil 2^{m-1} \rceil - 1} \sum_{p=\lceil 2^{m-2} \rceil}^{\lceil 2^{m-1} \rceil - 1} \sum_{q=0}^{\infty} \tag{B.15}$$

$$(-1)^q i^{n(2p+1)2^{2-m}} \frac{t^{\lceil 2^{m-1} \rceil q + n}}{(\lceil 2^{m-1} \rceil q + n)!}.$$

We will now change the p parameterization of the second summation, so it can be compared to the first.

$$\sum_{p=\lceil 2^{m-2} \rceil}^{\lceil 2^{m-1} \rceil - 1} (-1)^q i^{n(2p+1)2^{2-m}}$$

$$= \sum_{p=0}^{\lceil 2^{m-2} \rceil - 1} (-1)^q i^{n(2(p+\lceil 2^{m-2} \rceil)+1)2^{2-m}}$$

$$= \sum_{p=0}^{\lceil 2^{m-2} \rceil - 1} (-1)^q i^{n(2p+1)2^{2-m}} i^{2n} \tag{B.16}$$

$$= \sum_{p=0}^{\lceil 2^{m-2} \rceil - 1} (-1)^q i^{n(2p+1)2^{2-m}} (-1)^n$$

Update (B.15) with the re-parameterized second summation, using (B.16). This gives

$$\frac{1}{\lceil 2^{m-1} \rceil} \sum_{n=1}^{\lceil 2^{m-1} \rceil - 1} \sum_{p=0}^{\lceil 2^{m-2} \rceil - 1} \sum_{q=0}^{\infty}$$

$$(-1)^q i^{n(2p+1)2^{2-m}} \frac{t^{\lceil 2^{m-1} \rceil q + n}}{(\lceil 2^{m-1} \rceil q + n)!} +$$

$$\frac{1}{\lceil 2^{m-1} \rceil} \sum_{n=1}^{\lceil 2^{m-1} \rceil - 1} \sum_{p=0}^{\lceil 2^{m-2} \rceil - 1} \sum_{q=0}^{\infty} \tag{B.17}$$

$$(-1)^q i^{n(2p+1)2^{2-m}} (-1)^n \frac{t^{\lceil 2^{m-1} \rceil q + n}}{(\lceil 2^{m-1} \rceil q + n)!}.$$

The two summations differ only by a factor of $(-1)^n$. This means that the summations will cancel to zero for any odd n. So only even values of $n > 0$ could potentially contribute a nonzero sum to (B.11). We next show that values of $n > 0$ that are divisible by two sum to zero.

For even n, the summations in (B.17) will be equal, so we can add them to produce

$$\frac{1}{\lceil 2^{m-2} \rceil} \sum_{n=1}^{\lceil 2^{m-1} \rceil - 1} \sum_{p=0}^{\lceil 2^{m-2} \rceil - 1} \sum_{q=0}^{\infty}$$

$$(-1)^q i^{n(2p+1)2^{2-m}} \frac{t^{\lceil 2^{m-1} \rceil q + n}}{(\lceil 2^{m-1} \rceil q + n)!}. \tag{B.18}$$

We now repeat the procedure of splitting the p summation in two, then re-parameterizing p for the second summation. This gives us

$$\frac{1}{\lceil 2^{m-2} \rceil} \sum_{n=1}^{\lceil 2^{m-1} \rceil - 1} \sum_{p=0}^{\lceil 2^{m-3} \rceil - 1} \sum_{q=0}^{\infty}$$

$$(-1)^q i^{n(2p+1)2^{2-m}} \frac{t^{\lceil 2^{m-1} \rceil q + n}}{(\lceil 2^{m-1} \rceil q + n)!} +$$

$$\frac{1}{\lceil 2^{m-2} \rceil} \sum_{n=1}^{\lceil 2^{m-2} \rceil - 1} \sum_{p=0}^{\lceil 2^{m-3} \rceil - 1} \sum_{q=0}^{\infty} \tag{B.19}$$

$$(-1)^q i^{n(2p+1)2^{2-m}} i^n \frac{t^{\lceil 2^{m-1} \rceil q + n}}{(\lceil 2^{m-1} \rceil q + n)!}.$$

Equation (B.17) showed that odd values of n sum to zero; (B.19) shows in addition that if n contains an odd number of factors of 2 the summation will be zero.

This process can be repeated a total of $m-1$ times to show that all values of $n > 0$ sum to zero. This is sufficient to prove (B.3).

APPENDIX C
PROOF OF GENERALIZED EULER'S FORMULA GEOMETRIC INTERPRETATION

It will be proved that

$$e^{ti^{(2^{2-m})}} = e^{t \cos(\pi 2^{1-m})} e^{it \sin(\pi 2^{1-m})}. \tag{C.1}$$

Using the well-known identity $e^{i\pi/2} = i$ that arises from the standard Euler's formula, the term

$$i^{(2^{2-m})} = (e^{i\pi/2})^{(2^{2-m})} \tag{C.2}$$

can replaced in the generalized Euler's formula leading to

$$e^{ti^{(2^{2-m})}} = e^{t(e^{i\pi/2})^{(2^{2-m})}} \qquad \text{(C.3)}$$

Invoking the standard Euler's formula to break apart the upper exponent results in

$$e^{i\pi(2^{1-m})} = \cos(\pi 2^{1-m}) + i\sin(\pi 2^{1-m}). \qquad \text{(C.4)}$$

Substituting (C.4) into (C.3) leads to

$$e^{ti^{(2^{2-m})}} = e^{t(\cos(\pi 2^{1-m}) + i\sin(\pi 2^{1-m}))}, \qquad \text{(C.5)}$$

which finally is converted to

$$e^{ti^{(2^{2-m})}} = e^{t\cos(\pi 2^{1-m})}e^{it\sin(\pi 2^{1-m})}. \qquad \text{(C.6)}$$

Luciano Leonel Mendes received the BSc. and MSc. in Electrical Engineer from Inatel, Brazil in 2001 and 2003, respectively. In 2007 he received the Doctor in Electrical Engineer degree from Unicamp, Brazil. Since 2001 he is a professor at Inatel, Brazil, where he has acted as technical manager of the hardware development laboratory from 2006 to 2012. He has coordinated the Master Program at Inatel and several research projects funded by FAPEMIG, FINEP and BNDES. He was a visiting research, sponsored by CNPq-Brasil, at Vodafone Chair Mobile Communications Systems at the TU Dresden from 2013 until 2015.
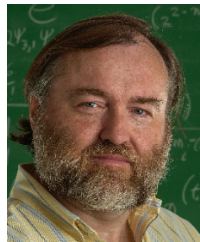
Jerrold Prothero received the B.Sc. degree in Physics (with honors) and Computer Science, the M.S.E. degree in Inter-Disciplinary Engineering, and the Ph.D. degree in Mechanical Engineering, all from the University of Washington, Seattle, U.S.A., in 1986, 1993, and 1998, respectively. His master's thesis introduced a new method for treating Parkinson's disease akinesia using virtual images, and his Ph.D. dissertation introduced a new approach to studying the psychophysics of virtual environments, as well as techniques for ameliorating simulator sickness. He has consulted widely on a range of technology issues. His mathematical interests led to a new generalization of Euler's formula and to the discovery of instantaneous spectral analysis. He founded and is CEO of Astrapi, which received its first significant funding in 2013, in order to commercialize a new approach to communication based on the generalized Euler's formula.

Jon Barrueco received the M.S. degree in Telecommunications Engineering from the Bilbao Engineering College, University of the Basque Country, in 2013. Since 2013 he is part of the TSR (Radiocommunications and Signal Processing) research group at the University of the Basque Country, where he is currently a PhD student involved in several research projects in the Signal Processing area for Wireless Communications. He is currently an active participant in the standardization process of the next-generation terrestrial broadcasting standard ATSC 3.0.

KM Zahidul Islam received the B.Sc. degree in Electrical and Electronic Engineering from Bangladesh University of Engineering and Technology (BUET), Dhaka, Bangladesh in 2003, and the MSEE and Ph.D. degrees in Electrical Engineering from The University of Texas at Dallas (UTD), Texas, USA in 2006 and 2011, respectively. In 2003, Dr. Islam joined the Department of Computer Science and Engineering at The University of Asia Pacific (UAP), Dhaka, Bangladesh as a Lecturer. Since May 2005, he has been with the Department of Electrical Engineering at UTD as a graduate student, later continued for Ph.D. degree. Dr. Islam joined Astrapi Corporation, Texas, USA on August 2015. Currently, he is with SpaceX, Redmond, USA.

Henry Douglas Rodrigues received the BSc. and MSc. in Electrical Engineer from Inatel, Brazil, in 2003 and 2008, respectively. He received his Ph.D. in Electrical Engineer at Unifei, Brazil, 2017. In 2001 he joined Hitachi Kokusai Linear, as an R&D engineer on digital bradcasting systems, became project manager in 2011, and chief engineer in 2013. He contributed for the developement of high efficiency RF power amplifiers, modulators, multiplexers, and power amplifier linearization with digital pre-distortion. Since 2016 he is with Inatel, Brazil, as a rivrcher on physical layer solutions for 5G networks.

Jon Montalban received the M.S. Degree and PhD in Telecommunications Engineering from the University of the Basque Country (Spain), in 2009 and 2014, respectively. Since 2009 he is part of the TSR (Radiocommunications and Signal Processing) research group at the University of the Basque Country, where he is currently a postdoctoral researcher involved in several projects in the Digital Terrestrial Television broadcasting area.

REFERENCES

[1] D. Schneider, "A faster fast fourier transform," *IEEE Spectrum*, vol. 49, no. 3, pp. 12–13, March 2012. doi: 10.1109/MSPEC.2012.6156851

[2] J. B. Allen and L. R. Rabiner, "A unified approach to short-time fourier analysis and synthesis," *Proceedings of the IEEE*, vol. 65, no. 11, pp. 1558–1564, Nov 1977. doi: 10.1109/PROC.1977.10770

[3] D. Gabor, "Theory of communication," *Electrical Engineers - Part I: General, Journal of the Institution of*, vol. 94, no. 73, pp. 58–, January 1947. doi: 10.1049/ji-1.1947.0015

[4] J. Ville, "Theorie et Applications de la Notion de Signal Analytique," *Cables et Transmission*, vol. 1, pp. 61–74, 1948.

[5] C. H. Page, "Instantaneous power spectra," *Journal of Applied Physics*, vol. 23, no. 1, pp. 103–106, 1952. doi: 10.1063/1.1701949

[6] L. Cohen, "Time-frequency distributions-a review," *Proceedings of the IEEE*, vol. 77, no. 7, pp. 941–981, Jul 1989. doi: 10.1109/5.30749

[7] S. Srinidhi, J. Proakis, and D. Manolakis, *Digital Signal Processing: Principles, Algorithms, and Applications. Solutions manual*. Prentice Hall, 1996. ISBN 9780133758337. [Online]. Available: https://books.google.com.br/books?id=iuLTPQAACAAJ

[8] A. V. Oppenheim, R. W. Schafer, and J. R. Buck, *Discrete-time Signal Processing (2Nd Ed.)*. Upper Saddle River, NJ, USA: Prentice-Hall, Inc., 1999. ISBN 0-13-754920-2

[9] V. Pulkki, S. Delikaris-Manias, and A. Politis, *Time–Frequency Processing: Methods and Tools*. IEEE, 2018. [Online]. Available: https://ieeexplore.ieee.org/xpl/articleDetails.jsp?arnumber=8320480

[10] S. L. Marple, "Time-frequency signal analysis: issues and alternative methods," in *Proceedings of the IEEE-SP International Symposium on Time-Frequency and Time-Scale Analysis (Cat. No.98TH8380)*, Oct 1998. doi: 10.1109/TFSA.1998.721427 pp. 329–332.

[11] J. Allen, "Short term spectral analysis, synthesis, and modification by discrete fourier transform," *IEEE Transactions on Acoustics, Speech, and Signal Processing*, vol. 25, no. 3, pp. 235–238, June 1977. doi: 10.1109/TASSP.1977.1162950

[12] S. Liu, J. Jiang, Y. Zhang, and J. Zhang, "Generalized fractional fourier transforms," *Journal of Physics A: Mathematical and General*, vol. 30, no. 3, p. 973, 1997. [Online]. Available: http://stacks.iop.org/0305-4470/30/i=3/a=020

[13] L. B. Almeida, "The fractional fourier transform and time-frequency representations," *IEEE Transactions on Signal Processing*, vol. 42, no. 11, pp. 3084–3091, Nov 1994. doi: 10.1109/78.330368

[14] B. Boashash, *Time-Frequency Signal Analysis and Processing: A Comprehensive Review*. Academic Press, 2013. ISBN 9780123984999 0123984998

[15] W. Martin and P. Flandrin, "Wigner-ville spectral analysis of nonstationary processes," *IEEE Transactions on Acoustics, Speech, and Signal Processing*, vol. 33, no. 6, pp. 1461–1470, December 1985. doi: 10.1109/TASSP.1985.1164760

[16] F. Hlawatsch and W. Krattenthaler, "Bilinear signal synthesis," *IEEE Transactions on Signal Processing*, vol. 40, no. 2, pp. 352–363, Feb 1992. doi: 10.1109/78.124945

[17] M. G. Amin, W. Mu, and Y. Zhang, "Improved time-frequency synthesis using array manifolds," in *Proceedings of the Sixth International Symposium on Signal Processing and its Applications (Cat.No.01EX467)*, vol. 1, Aug 2001. doi: 10.1109/ISSPA.2001.949800 pp. 158–161 vol.1.

[18] O. P. K. Douglas J. Nelson, "Invertible time-frequency representations," pp. 3461 – 3461 – 12, 1998. [Online]. Available: https://doi.org/10.1117/12.325676

[19] C. E. Shannon, "Communication in the presence of noise," *Proc. Institute of Radio Engineers*, vol. 37, no. 1, pp. 10–21, 1949.

[20] J. Prothero, "Spiral polynomial division multiplexing," Sep. 9 2018, uS Patent 10,069,664 B2. [Online]. Available: https://patents.google.com/patent/US10069664B2

[21] J. Cairns, "Geometrically modulated waves," Jan. 1 1994, uS Patent 5,920,238. [Online]. Available: https://patents.google.com/patent/US6204735

[22] ——, "Geometrically modulated waves," Oct. 8 1996, uS Patent 5,563,556. [Online]. Available: https://www.google.com/patents/US5563556

[23] J. Prothero, "Telecommunication signaling using nonlinear functions," Sep. 26 2013, uS Patent App. 13/902,502. [Online]. Available: https://www.google.com.br/patents/US20130251018

[24] J. Prothero and N. Jones, "Methods and systems for communicating," Oct. 18 2012, uS Patent App. 13/447,641. [Online]. Available: https://www.google.com.br/patents/US20120263031

[25] N. Jones and J. Prothero, "Software defined radio," Mar. 31 2015, uS Patent 8,995,546. [Online]. Available: https://www.google.com.br/patents/US8995546